# Biocompatible poly(catecholamine)-film electrode for potentiometric cell sensing.

Taira Kajisa*[†], Yoshiyuki Yanagimoto[†], Akiko Saito[‡], and Toshiya Sakata *[‡]

† *PROVIGATE Inc., Entrepreneur Plaza, The University of Tokyo, 7-3-1 Hongo, Bunkyo-ku, Tokyo 113-0033, Japan*

‡ *Department of Materials Engineering, School of Engineering, The University of Tokyo, 7-3-1 Hongo, Bunkyo-ku, Tokyo 113-8656, Japan.*

*KEYWORDS: biomimetic material, poly(catecholamine), pH-sensitive biosensor, voltage follower circuit, cell sensing.*

**ABSTRACT:** Surface-coated poly(catecholamine) (pCA) films have attracted attention as biomaterial interfaces owing to their biocompatible and physicochemical characteristics. In this paper, we report that pCA-film-coated electrodes are useful for potentiometric biosensing devices. Four different types of pCA film—L-dopa, dopamine, norepinephrine, and epinephrine—with thicknesses in the range of 7–27 nm were electropolymerized by oxidation on Au electrodes by using cyclic voltammetry. By using the pCA-film electrodes, the pH responsivities were found to be 39.3 to 47.7 mV/pH within the pH range of 1.68 to 10.01 on the basis of the equilibrium reaction with hydrogen ions and the functional groups of the pCAs. The pCA films suppressed nonspecific signals generated by other ions ($Na^+$, $K^+$, $Ca^{2+}$) and proteins such as albumin. Thus, the pCA-film electrodes can be used in pH-sensitive and pH-selective biosensors. HeLa cells were cultivated on the surface of the pCA-film electrodes to monitor cellular activities. The surface potential of the pCA-film electrodes changed markedly because of cellular activity; therefore, the change in the hydrogen ion concentration around the cell/pCA-film interface could be monitored in real time. This was caused by carbon dioxide or lactic acid that is generated by cellular respiration and dissolves in the culture medium, resulting in the change of hydrogen concentration. pCA-film electrodes are suitable for use in biocompatible and pH-responsive biosensors, enabling the more selective detection of biological phenomena.

Biomimetic materials have received considerable interest as synthetic materials inspired by the structures, properties, or functions of natural materials and living matter. Marine mussels are well known for easily adhering to and covering wave-washed rocks by secreting L-3,4-dihydroxyphenylalanine (L-dopa or LD).[1] Imitating the adhesive behavior of mussels, catecholamines (CAs) such as LD have been utilized for the surface modification of metal and metal oxide substrates by a simple dip-coating method.[2-7]

CAs play an important role in the field of neurobiology as neurotransmitters and hormones. Each CAs was sequentially metabolized by the conversion of tyrosine to biologically important derivatives, such as LD, dopamine (DA), norepinephrine (NE, also called noradrenaline), and epinephrine (EP, also called adrenaline), by enzymatic reactions in the metabolic pathway. These derivative CAs have similar chemical structures but different functional groups. Furthermore, CAs are polymerized by self-oxidation, forming indole moieties that act as monomers for self-polymerization.[8,9] The surface modification of poly-CAs (pCAs) renders substrate surfaces with hydrophilicity, making it possible to graft functional chemicals using the Michael addition and Schiff base reaction.[10] As an example of pCAs application, it was reported about poly-NE (pNE) fibers that were developed for a 2D tissue culture substrate and have been reported as a functional bio-interface for neuronal differentiation.[11]

Bioinspired materials are required at the signal-transduction-interface of biosensors as they enhance the detection sensitivity, selectivity, and biocompatibility around a bio/sensor interface. A biologically coupled gate field-effect transistor (FET), a biosensor, is based on a potentiometric method of directly detecting ionic charges, which enables the simple analysis of biomolecular recognition events and cellular activities in a label-free and noninvasive manner.[12-17] The surface modification of the gate electrode improves the electrical properties of FET biosensors by forming functional interfaces on the gate surface, such as self-assembled monolayers, oligonucleotide probes, and hydrogels.[18-21] The gate electrode can be extended and separated from the gate of a metal-oxide-semiconductor FET. Therefore, the device structure of the extended-gate electrode makes it possible to easily modify functional molecules on the gate electrode, whose materials can be selected in accordance with its use. However, the effect of a pCA-film on the electrical signal has not yet been investigated for potentiometric biosensors.

In this study, we investigated the electrical properties of pCA-film electrodes for potentiometric biosensing by using a surface potential detector. pCA films were polymerized by self-oxidation using cyclic voltammetry, and the changes in the surface potential of the electrodes caused by pH and in the presence of other cations and albumin were evaluated. Using the pH responsivities of the pCA-film electrodes, cellular activities such as respiration that resulted in a change in pH around the cell/pCA-film interface were monitored in real time.

## Experimental Section

### Materials

LD, DA, NE, and EP were purchased from Tokyo Chemical Industries (Japan). Tris hydroxy aminomethane and pH standard solution from pH 1.68 to 10.01 were purchased from Wako Pure Chemical Industries (Japan). Dulbecco's Modified Eagle Medium (DMEM, +10% FBS) for cell culture was purchased from Invitrogen (U.S.A.).

### Fabrication of poly(catecholamine)-modified Au electrode

An Au electrode was fabricated by sputtering. First, Cr (thickness 15 nm) was sputtered as an adhesion layer. Afterwards, the gold electrode (thickness 100 nm) was sputtered. A 10-mm-diameter glass ring was attached to the Au substrate by using epoxy resin or poly(dimethylsiloxane). Au substrates were modified by each type of pCA using electropolymerization. 500 μL solutions of 25 mM LD and DA solution were prepared by dissolving them in a $N_2$-bubbled 100-mM Tris buffer (pH 10.4). NE was prepared using the same buffer, and 2 μL of 2 mM HCl was then dissolved into the prepared NE. Similarly, EP was prepared by dissolving 2 μL of 1 M HCl into the buffer. Each CA was oxidized using cyclic voltammetry (ALS614E, BAS) with an AgCl electrode as a reference electrode and platinum as a counter electrode. The Au electrode in each CA solution was oxidized by sweeping the potential from −0.5 to +0.5 V at a scan rate of 0.02 V/s. The sweep was repeated for 30 cycles, after which the current saturated. After electropolymerization, the Au electrode was washed with ethanol and dried in a vacuum. The static water contact angle was measured at the surface of each pCA-modified Au electrode by using a CA-W automatic contact-angle meter (Kyowa Interface Science Co., Ltd., Japan). 2 μL drops of ultrapure water were placed on the surface of each pCA-modified Au electrode at room temperature. The water droplets were monitored with a charge-coupled device camera, and the captured images were analyzed using FAMAS software (Kyowa Interface Science) to determine the static contact angle. The contact angle was calculated as the average value from five images taken at different positions.

### Estimation of poly(catecholamine) thickness on the Au surface by ellipsometric analysis

The thickness of each type of electropolymerized pCA was calculated by ellipsometric measurement using a rotating ellipsometer (model M2000U, J.A. Woollam Co., Inc., U.S.A.) and WVASE32 software. The wavelength of incident light ranged between 193 and 1690 nm, and the angle of incidence was 65°, 70°, 75°, or 80°. To calculate the layer thickness, the experimental data spectrum was fitted using the Cauchy model, where the dispersion of the refractive index was approximated. The ellipsometric measurement was performed three times for each type of pCA, and the thickness was calculated as the average of the three measurements.

### Change in surface potential of pCA-film electrodes using a surface potential detector

Each type of pCA-modified Au electrode was connected to a surface potential detector (SPD) by a crocodile clip, and the change in each CA surface potential was measured with a real-time monitoring system developed by Komatsu Electronics and PROVIGATE. The SPD was constructed from a voltage follower circuit, which is a noninverting amplifier circuit of a CMOS operational amplifier (AD8609, Analog Devices, Japan) with the standard potential adjusted to 2.5 V using an AgCl electrode as a reference electrode. The analog output signal was converted to a digital signal using RAI-16 software (Elmos, Japan). A schematic illustration of the pCA-modified SPD and its circuit is shown in Figure 1A and the chemical structure of each pCA is shown in Figure 1B. To confirm the response to hydrogen ions, the pH of the standard pH solution was changed from 1.68 to 10.01 then returned to 1.68. To observe the ion concentration dependence, 0.1, 1, 10, 100, and 1000 mM of sodium chloride, potassium chloride, and calcium chloride solutions were adjusted using 100 mM of HEPES buffer (pH 7.4) via titration. Similar concentrations of sodium hydroxide and potassium hydroxide were used in the respective cases wherein potassium and calcium ion solutions and sodium ion solution were used. To ascertain the effect of albumin and dopamine during real-time monitoring, 500 μL of phosphate buffered saline (PBS, pH 7.4, Invitrogen) buffer was poured into the glass ring of each pCA-modified Au electrode. Then, 5 μL of either 100 or 500 mg/ml albumin diluted with PBS buffer was added to examine the effect of output voltage noise caused by the addition (the final concentration was 1 or 5 mg/ml, respectively). 5 μL of 100 nM to 100 μM of dopamine diluted with PBS buffer was added in the same manner.

### Measurement of cellular activity using pCA-film electrodes

To investigate cell sensing using the pCA-modified Au SPD, HeLa cells were cultured on each pCA-modified Au electrode and connected to the SPD using a platinum electrode as the reference electrode at 37°C in an incubator system (ASTEC Co., Ltd., Japan) containing 5% $CO_2$. DMEM (+10% FBS, 100 U/mL of Penicillin, and 100 μg/mL of Streptomycin) was used as the culture medium. The cells were seeded on each 10 mmΦ electrode in 400 μL of the culture medium at a concentration of approximately $1 \times 10^5$ cells/ml. After incubation for 24 h to promote adhesion to the pCA substrate and induce the proliferation phase, real-time monitoring of the surface potential in each pCA-modified Au SPD was performed in the incubator under conditions suitable for cell culture. Considering the various factors that contribute to background noise, such as nonspecific adsorption and small changes in the culture solution pH, the actual cell respiratory activity was evaluated from the differences in the potential between the cell cultures with cells, with fixed-cells, and without cells by using three identical devices.

## Results and Discussion

### Fabrication of a thin layer pCA on Au electrodes using cyclic voltammetry

To investigate the electrical properties of the pCA films, four different pCA films were deposited by electropolymerization on Au electrodes using cyclic voltammetry. The Au electrodes were oxidized by sweeping from −0.5 to +0.5 V in deoxidized alkaline solutions, each including 25 mM of one of the four CAs. Figure 2 shows the cyclic voltammograms for each CA. The voltage sweep was repeated 30 times in the forward direction. As the swept voltage increased, anodic current began to flow. Thus, in the first few sweep cycles, a minimum current was observed at approximately +0.5 V [ca. $-5.0 \times 10^{-4}$ A/cm$^2$ in LD (Fig. 2A), ca. $-2.5 \times 10^{-4}$ A/cm$^2$ in DA (Fig. 2B), ca. $-5.0 \times 10^{-4}$ A/cm$^2$ in NE (Fig. 2C), and ca. $-5.0 \times 10^{-4}$ A/cm$^2$ in EP (Fig. 2D)], and another negative peak was ob-

served at approximately +0.2 V [ca. $-4.5 \times 10^{-4}$ A/cm$^2$ in LD (Fig. 2A), ca. $-2.2 \times 10^{-4}$ A/cm$^2$ in DA (Fig. 2B), ca. $-4.0 \times 10^{-4}$ A/cm$^2$ in NE (Fig. 2C), and ca. $-1.7 \times 10^{-4}$ A/cm$^2$ in EP (Fig. 2D)]. As a representative model of the pCA formation process, Scheme 1 shows a proposed mechanism for the oxidative polymerization of DA. There are three steps in the oxidative polymerization of DA. First, DA is oxidized to dopaminequinone. Next, 5,6-dihydroxyindole is generated from leukodopamine chrome. Finally, 5,6-dihydroxyindole is oxidized, resulting in self-polymerization.[22-24] Two electrons are denoted to the Au electrode in each step. The oxidative process can be conceptually regarded as two steps: (1) the conversion to the indole moiety, and (2) the conversion to the polymer. Thus, the distinctive features of the anodic current near 0.2 and 0.5 V reflect the oxidation process to the indole monomer and the polymerization process, respectively. The polymerization of the oxidized indole derivative was expected after the preparation of the monomers. As the cycle number increased, the anodic current decreased, until no further change was seen after 20 cycles, suggesting that the concentration of CAs during film deposition reached a saturated condition or that the thickness of the insulated CA-films increased.

**Characterization of pCA films on Au substrate**

To evaluate the properties of the pCA films, their thicknesses were calculated by fitting to the optical model using an ellipsometer (Figure S1 in Supporting Information). The thicknesses were 7.1 ± 0.4 nm in pLD, 23.1 ± 1.4 nm in pDA, 26.5 ± 1.3 nm in pNE, and 10.1 ± 0.3 nm in pEP. The pDA and pNE films were thicker than the pLD and pEP films. This result can be explained using the cyclic voltammograms shown in Figure 2. In DA and NE, the anodic current gradually reached approximately to zero at positive voltages with increasing number of cycles, whereas the anodic current continued to flow in LD and EP even after 30 cycles. This means that the deposition rates of the pCA films by the electropolymerization process were different. This was due to the different chemical structures of the CAs. LD and EP have slightly longer molecular chains than DA and NE, which may suppress the formation of the indole moiety, i.e., the monomer for polymerization. Therefore, the chemical structures of LD and EP were more difficult to convert to indole derivatives than DA and NE, resulting in a delay of the polymerization. In contrast, pCA films produced by self-oxidative polymerization, which were incubated in an alkaline solution at room temperature for 24 h, had greater thicknesses than those by electropolymerization in the range of 50–70 nm, except for the pEP film, which had a thickness of 20 nm (data not shown). It was previously reported that the thickness of a pDA film formed by self-oxidation reached 50 nm after 24 h.[1] Consequently, pCA films can be designed by controlling the oxidation time or the electrochemical conditions.

The surfaces of the electropolymerized pCA films were also characterized by measuring the static water contact angle. The static water contact angles for the pCA-film surfaces were 56.1° ± 1.6° for pLD, 69.0° ± 1.7° for pDA, 65.2° ± 2.7° for pNE, and 59.2° ± 0.9° for pEP (Figure S2 in Supporting Information). The surface modification of the Au electrodes by the pCA films contributed to the enhanced hydrophilicity when compared with the nonmodified Au surface, whose contact angle was 87.3° ± 0.7°.

**pH responsivity of pCA-film electrodes**

The change in the surface potential ($\Delta V_{out}$) of the pCA films with pH was investigated in a real time, as shown in Figure 3. The potential response of each pCA-film surface was determined for a reversible change in pH of between 1.68 and 10.01, using the circuit shown in Figure 1A. $\Delta V_{out}$ for the pCA-film electrodes gradually shifted in the negative direction when the pH was increased from 1.68 to 10.01, but it recovered in a stepwise manner to the original value when the pH was decreased to its initial value of 1.68. Interestingly, $\Delta V_{out}$ for the pCA films continued to return to its original value even after the biosensor device was immersed in solutions of differing pH. The pEP-film electrode was an exception and did not fully recover its initial $\Delta V_{out}$. Compared with other catecholamines, the amino terminal group, which is responsible for the equilibrium with the hydrogen ions, was capped by a methyl group in pEP. Thus, the pEP-coated Au electrode was less sensitive to the pH reaction. The pH responsiveness of pCA-film electrodes was stable in a wide range of pH solutions and during long-term measurements because of the strong adhesiveness of pCA to metals and polymer chains via various adhesive mechanisms, such as π-π stacking, hydrogen bonding, cation-π, and electrostatic interactions. From the pH responses shown in Figure 3A, the gradients of the calibration curves of $\Delta V_{out}$ against pH were calculated to be 45.8 mV/pH ($R^2 = 0.992$) for pLD, 43.9 mV/pH ($R^2 = 0.987$) for pDA, 47.7 mV/pH ($R^2 = 0.993$) for pNE, and 39.3 mV/pH ($R^2 = 0.988$) for pEP, as shown in Figure 3B. Thus, the pH responsivities of the pCA-film electrodes arose from the equilibrium reaction of hydrogen ions with the functional groups of the pCAs and were dependent upon the chemical structure of pCAs. The following shows the equilibrium reactions for the phenolic hydroxyl group (eq. 1), amino group (eq. 2), and carboxyl group (eq. 3);

$$C_6H_5\text{-}OH \rightleftarrows C_6H_5\text{-}O^- + H^+ \quad \text{(eq. 1)},$$

$$\text{-}NH_2 + H^+ \rightleftarrows NH_3^+ \quad \text{(eq. 2)},$$

$$\text{-}COOH \rightleftarrows \text{-}COO^- + H^+ \quad \text{(eq. 3)}.$$

Although the pCA-film electrodes resulted in pH responsivities, $\Delta V_{out}$ for the pEP film was typically not observed in alkaline solutions. This means that the size of the signal shift may depend on the type of functional group and level of p*K*a in the measurement solution. As can be seen from their chemical structures, the pLD and the pNE films comprised not only diol and amino groups like the pDA film but also other groups (carboxyl groups for the pLD film or hydroxyl groups for the pNE film) that contributed to the interaction with hydrogen ions based on the equilibrium reactions. Therefore, the pLD- and pNE-film electrodes produced larger electrical signals than the pDA- and pEP-film electrodes. This contributed to the interaction with hydrogen ions and each functional group at each pH. Thus, the pLD- and pNE-film electrodes produced larger electrical signals than the pDA- and the pEP-film electrodes.

The effect of other ions on the electrical signals of the pCA-film electrodes was investigated in salt solutions of NaCl, KCl, and $CaCl_2$ with concentrations in the range of 100 μM to 1 M at a constant pH of 7.4. Figure 4 shows $\Delta V_{out}$ for various salt concentrations. As shown in Figure 4A, $\Delta V_{out}$ decreased slightly at approximately 5 mV/p$Na^+$ for the pLD-, pNE-, and pEP-film electrodes and at approximately 10 mV/p$Na^+$ for the pDA-film electrode in a range of NaCl concentrations from 10 mM to 1 M. No such changes were observed at concentrations of less than 10 mM for any of

the electrodes. Similarly, $\Delta V_{out}$ barely varied with KCl concentration but decreased slightly at higher concentrations, as shown in Figure 4B. Thus, the negative shift of $\Delta V_{out}$ indicates an increase in the numbers of negative charges at the pCA-film surfaces. Therefore, $\Delta V_{out}$ at over 10 mM salt concentration in the NaCl and KCl solutions is attributable to the increase in the amount of chloride ions as counter anions, rather than an increase in the numbers of cations.[25,26] In contrast, $\Delta V_{out}$ markedly increased upon the addition of 1 M $CaCl_2$ for the pCA-film electrodes. Specifically, $\Delta V_{out}$ for the pLD-film electrode showed a large shift of approximately 33 mV (Figure 4C). This is because calcium ions were easily cross-linked with two carboxyl groups, which are known to exhibit a strong interaction owing to the chelate effect. $Na^+$, $K^+$, and $Ca^{2+}$ concentrations are maintained at around 150, 5, and 10 mM, respectively, in biological environments such as cell culture media and blood. Thus, the pH responsivities of the pCA-film electrodes were sufficiently large to eliminate the effect of changes in the $Na^+$, $K^+$, and $Ca^{2+}$ concentrations on electrical signals, under biological conditions.

To evaluate the effect of the pCA films on a nonspecific signal caused by the nonspecific adsorption of impurities such as proteins on Au electrodes, $\Delta V_{out}$ of the pCA-film electrodes was monitored by the addition of albumin and dopamine. It is well known that albumin easily binds to an Au surface owing to thiol-Au binding from cysteine residues of albumin.[27-29] $\Delta V_{out}$ for the nonmodified Au electrode markedly decreased by approximately 60 mV upon the addition of 1 mg/ml of albumin and, subsequently, decreased by over 100 mV upon the addition of 5 mg/ml of albumin. Conversely, the pCA-film electrodes barely exhibited any electrical response even upon the addition of 5 mg/ml of albumin, although $\Delta V_{out}$ for the pNE-film electrode slightly shifted in the negative direction (Figure S3 in Supporting Information). Moreover, the pCA-film electrodes suppressed nonspecific signals upon the addition of small molecules, such as dopamine (Figure S3). Therefore, the surface modification of Au surfaces by pCA films is expected to contribute to the prevention of unexpected signals caused by impurities in a biological sample. However, proteins may adhere to pCA films (see the next section). Thus, the interaction of albumin with Au surfaces may be prevented by the pCA films, meaning that the surface modification would not suppress nonspecific adsorption but only nonspecific signals. Finally, it was confirmed that the pCA films were hydrogen-ion sensitive even in different redox potential solutions, whereas the bare Au electrode responded to the changes in redox potential (Figure S4 in Supporting Information). The surface potentials of the pCA films did not respond to changes in the redox potential; however, the surface potential of bare Au improved in response to the redox potential.

### Real-time monitoring of cellular activity by cell cultivation on pCA-film electrodes

Cellular activities can be detected as a change in ion concentration around a cell/electrode interface using a potentiometric method. In this study, the pCA-film electrodes showed high selectivity for pH detection, meaning that the pH variation due to cellular functions, i.e., respiration, could be monitored by the pCA-film electrodes. Cellular respiration in some living cells has previously been observed, using potentiometric detection devices such as a pH-responsive ion-sensitive FET (ISFET), as a change in pH.[30] This is because pH variation is induced around a cell/gate interface by the dissolution of carbon dioxide or lactic acid, caused by cellular metabolism.[31-33] In this study, HeLa cells were cultivated on the surface of each pCA film, and then $\Delta V_{out}$ for the pCA-film electrodes was monitored using the SPD in order to measure the changes in pH from $\Delta V_{out}$ calculation. HeLa cells were proliferated from $1.7 \times 10^5$ cells/ml to $5.0 \times 10^5$ cells/ml during 24 h of the measurement (Figure 5A). Figure 5B shows the images of HeLa cell at 0 h (left) and 24 h (right) of measurement time, and the time course for the change in the surface potential on each pCA film with cells, with fixed cells, and without cells in DMEM with 10% FBS over 24 h are shown in Figure 5C. $\Delta V_{out}$ for the pCA-film electrodes with cells clearly increased with the growth and proliferation of the cultured cells, and then saturated within 24 h due to the confluently cultured cells. In contrast, $\Delta V_{out}$ of electrodes with fixed cells increased slowly and linearly, but less rapidly than that of electrodes with non-fixed cells, whereas that of electrodes without fixed cells barely changed. Regarding the smaller increase of $\Delta V_{out}$ in the case of fixed cells, it may be because of water entering through the gap between the cell and the substrate during the 24 hours of monitoring, thus slowly increasing the capacitance at the interface of the electrode. Thus, the pH variation around the cell/pCA-film interface, which was caused by cellular activities, was monitored in real time, because the pCA-film electrodes were very pH responsive. From the results in Figure 5C, the difference in the signals for the pCA-film electrodes with and without HeLa cells, after 24 h, was calculated as 46 mV for pLD, 38 mV for pDA, 47 mV for pNE, and 34 mV for pEP, as shown in Figure 5D. Considering the pH responsivities for the pCA-film electrodes shown in Fig. 3, the pH around the cell/electrode interface changed from approximately 7.4 to 6.4 in every electrode, after 24 h of cultivation. Using ISFET, which had a lower detection limit of approximately 60 mV/pH, the pH changed from 7.4 to 6.1 in the same culture system, as indicated by the approximate 80-mV gate potential shift (Fig. S5 in the Supporting Information). The difference in the detection ability of pCA-film electrodes and ISFET is derived from the difference in the number of functional groups contributing to the equilibrium of the hydrogen ions. Moreover, the difference in the calculated pH shift between them may have been due to the type of the substrate material. We attributed the difference between the metal oxide surface in ISFET and the pCAs surface in the pCA-film electrodes to the cells' condition, such as their adhesiveness and growth rate during the cultivation. Taking these factors into consideration, however, the potential shift during the cell cultivation with the pCA-film electrode corresponded well with that obtained using ISFET, although differences were observed.

Regarding the adhesion of cells on the pCA film, it has been reported that neuronal cells can be cultivated on a pNE fiber which acted as a 2D tissue culture substrate and helped to promote cell differentiation.[11] HeLa cells adhered to all the pCA-film surfaces in this study. It seems that a number of proteins must adhere to the pCA films, becoming a scaffold for cells. It was previously reported that some proteins in a culture medium adhered to pCAs on substrates because the hydroxyl groups in the pCAs were covalently bound to amino groups at the protein surfaces.[1,34,35] Thus, the pCA-film electrodes in this study promoted adhesion of proteins as a scaffold for cells, and enabled the potentiometric detection of pH variation caused by cellular activities.

### Conclusion

In this study, we verified that pCA-film-coated electrodes are useful in potentiometric biosensing devices. Four different pCA

films—L-dopa, dopamine, norepinephrine, and epinephrine—were electropolymerized by oxidation on Au electrodes using cyclic voltammetry with thicknesses between 7–27 nm. The pH responsivities of the pCA-film electrodes were found to be 39.3–47.7 mV/pH within the pH range of 1.68 to 10.01, depending on the equilibrium of functional groups at the surface of the pCA films with hydrogen ions. The pCA films suppressed nonspecific signals based on other ions ($Na^+$, $K^+$, $Ca^{2+}$) and proteins such as albumin. Thus, the pCA-film electrodes can be used in pH-sensitive and selective biosensors. HeLa cells were cultivated on the surface of the pCA-film electrodes to monitor cellular activities. The surface potential of the pCA-film electrodes changed markedly because of cellular activities, and the change in the hydrogen ion concentration around the cell/pCA-film interface was monitored in real time. This is because carbon dioxide or lactic acid generated by cellular respiration dissolved in the culture medium, resulting in hydrogen ion variation. Platforms based on pCA-film electrodes should be suitable for use as biocompatible and pH-responsive biosensors, which will enable the more selective detection of biological phenomena upon further surface modifications of the pCA films.

## ASSOCIATED CONTENT

The Supporting Information is available free of charge on the ACS Publications website at DOI: xxxxxxxxxx

Additional figures: Ellipsometric spectra, Static contact angles, Suppression effect of albumin and dopamine by pCA, Time course for the differential interfacial voltage changes of ion-sensitive FET. (PDF)

## AUTHOR INFORMATION


### Corresponding Author

*Taira Kajisa

PROVIGATE Inc, Univ. of Tokyo Entrepreneur Plaza, 7-3-1 Hongo, Bunkyo-ku, Tokyo 113-0033, Japan

E-mail: kajisa@provigate.com; Tel: +81-3-5615-8285

*Toshiya Sakata

Department of Materials Engineering, School of Engineering, The University of Tokyo, 7-3-1 Hongo, Bunkyo-ku, Tokyo 113-8656, Japan

E-mail: sakata@biofet.t.u-tokyo.ac.jp; Tel: +81-3-5841-1842

### ORCID

Taira Kajisa: 0000-0001-6121-9274

Toshiya Sakata: 0000-0002-5153-2555


### Notes

The authors declare no competing financial interest.

### Author Contributions

T. K., Y. Y. and T. S. are co-first authors.

## ACKNOWLEDGMENT

Part of this work was conducted at the Advanced Characterization Nanotechnology Platform of the University of Tokyo, supported by the "Nanotechnology Platform" of the Ministry of Education, Culture, Sports, Science and Technology (MEXT), Japan. The authors wish to thank Assistant Professor K. Konishi of the University of Tokyo in Japan for his help in the ellipsometry experiment. This study was partly supported by the New Energy and Industrial Technology Development Organization (NEDO) under the Ministry of Economy Trade and Industry (METI) of Japan [grant number: 0105001]. The authors would like to thank Enago (www.enago.jp) for the English language review.

## REFERENCES


1. Lee, H.; Dellatore, S. M.; Miller, W. M.; Messersmith, P. B. Mussel-inspired surface chemistry for multifunctional coatings. *Science* **2007**, 318 (5849), 426-430.

2. Franzmann, E.; Khalil, F.; Weidmann, C.; Schroder, M.; Rohnke, M.; Janek, J.; Smarsly, B. M.; Maison, W. A biomimetic principle for the chemical modification of metal surfaces: Synthesis of tripodal catecholates as analogues of siderophores and mussel adhesion proteins. *Chemistry* **2011**, 17 (31), 8596-8603.

3. Jiang, J.; Zhu, L.; Zhu, L.; Zhu, B.; Xu, Y. Surface characteristics of a self-polymerized dopamine coating deposited on hydrophobic polymer films. *Langmuir* **2011**, 27 (23), 14180-14187.

4. Ogaki, R.; Bennetsen, D. T.; Bald, I.; Foss, M. Dopamine-assisted rapid fabrication of nanoscale protein arrays by colloidal lithography. *Langmuir* **2012**, 28 (23), 8594-8599.

5. Du, X.; Li, L.; Li, J.; Yang, C.; Frenkel, N.; Welle, A.; Heissler, S.; Nefedov, A.; Grunze, M.; Levkin, P. A. Uv-triggered dopamine polymerization: Control of polymerization, surface coating, and photopatterning. *Adv. Mater.* **2014**, 26 (47), 8029-8033.

6. Fabregat, G.; Armelin, E.; Aleman, C. Selective detection of dopamine combining multilayers of conducting polymers with gold nanoparticles. *J. Phys. Chem. B* **2014**, 118 (17), 4669-4682.

7. Lim, C.; Huang, J.; Kim, S.; Lee, H.; Zeng, H.; Hwang, D. S. Nanomechanics of poly(catecholamine) coatings in aqueous solutions. *Angew. Chem. Int. Ed. Engl.* **2016**, 55 (10), 3342-3346.

8. Liebscher, J.; Mrowczynski, R.; Scheidt, H. A.; Filip, C.; Hadade, N. D.; Turcu, R.; Bende, A.; Beck, S. Structure of polydopamine: A never-ending story? *Langmuir* **2013**, 29 (33), 10539-10548.

9. Shi, L.; Santhanakrishnan, S.; Cheah, Y. S.; Li, M.; Chai, C. L.; Neoh, K. G. One-pot uv-triggered o-nitrobenzyl dopamine polymerization and coating for surface antibacterial application. *ACS Appl. Mater. Interfaces* **2016**, 8 (48), 33131-33138.

10. Huang, N.; Zhang, S.; Yang, L.; Liu, M.; Li, H.; Zhang, Y.; Yao, S. Multifunctional electrochemical platforms based on the michael addition/schiff base reaction of polydopamine modified reduced graphene oxide: Construction and application. *ACS Appl. Mater. Interfaces* **2015**, 7 (32), 17935-17946.

11. Taskin, M. B.; Xu, R.; Zhao, H.; Wang, X.; Dong, M.; Besenbacher, F.; Chen, M. Poly(norepinephrine) as a functional bio-interface for neuronal differentiation on electrospun fibers. *Phys. Chem. Chem. Phys.* **2015**, 17 (14), 9446-9453.

12. Bergveld, P. Development of an ion-sensitive solid-state device for neurophysiological measurements. *IEEE Trans. Biomed. Eng.* **1970**, 17 (1), 70-71.

13. Fromherz, P.; Offenhausser, A.; Vetter, T.; Weis, J. A neuron-silicon junction: A retzius cell of the leech on an insulated-gate field-effect transistor. *Science* **1991**, 252 (5010), 1290-1293.

14. Sakata, T.; Miyahara, Y. Potentiometric detection of single nucleotide polymorphism by using a genetic field-effect transistor. *ChemBioChem* **2005**, 6 (4), 703-710.

15. Sakata, T.; Miyahara, Y. Detection of DNA recognition events using multi-well field effect devices. *Biosens. Bioelectron.* **2005**, 21 (5), 827-832.

16. Sakata, T.; Miyahara, Y. DNA sequencing based on intrinsic molecular charges. *Angew. Chem. Int. Ed. Engl.* **2006**, 45 (14), 2225-2228.

17. Rothberg, J. M.; Hinz, W.; Rearick, T. M.; Schultz, J.; Mileski, W.; Davey, M.; Leamon, J. H.; Johnson, K.; Milgrew, M. J.; Edwards, M.; Hoon, J.; Simons, J. F.; Marran, D.; Myers, J. W.; Davidson, J. F.; Branting, A.; Nobile, J. R.; Puc, B. P.; Light, D.; Clark, T. A.; Huber, M.; Branciforte, J. T.; Stoner, I. B.; Cawley, S. E.; Lyons, M.; Fu, Y. T.; Homer, N.; Sedova, M.; Miao, X.; Reed, B.; Sabina, J.; Feierstein, E.; Schorn, M.; Alanjary, M.; Dimalanta, E.; Dressman, D.; Kasinskas, R.; Sokolsky, T.; Fidanza, J. A.; Namsaraev, E.; McKernan, K. J.; Williams, A.; Roth, G. T.; Bustillo, J. An integrated semiconductor device enabling non-optical genome sequencing. *Nature* **2011**, 475 (7356), 348-352.

18. Park, K. Y.; Kim, M. S.; Choi, S. Y. Fabrication and characteristics of mosfet protein chip for detection of ribosomal protein. *Biosens. Bioelectron.* **2005**, 20 (10), 2111-2115.

19. Sakata, T.; Matsumoto, S.; Nakajima, Y.; Miyahara, Y. Potential behavior of biochemically modified gold electrode for extended-gate field-effect transistor. *Jpn. J. Appl. Phys.* **2005**, 44 (4S), 2860-2863.

20. Kajisa, T.; Sakata, T. Fundamental properties of phenylboronic-acid-coated gate field-effect transistor for saccharide sensing. *ChemElectroChem* **2014**, 1 (10), 1647-1655.

21. Kajisa, T.; Sakata, T. Characterization of ion-sensitive extended-gate field effect transistor coated with functional self-assembled monolayer. *Jpn. J. Appl. Phys.* **2015**, 54 (4), 04DL06.

22. Lynge, M. E.; van der Westen, R.; Postma, A.; Stadler, B. Polydopamine--a nature-inspired polymer coating for biomedical science. *Nanoscale* **2011**, 3 (12), 4916-4928.

23. Dreyer, D. R.; Miller, D. J.; Freeman, B. D.; Paul, D. R.; Bielawski, C. W. Perspectives on poly (dopamine). *Chem.Sci.* **2013**, 4 (10), 3796-3802.

24. Ho, C.-C.; Ding, S.-J. Structure, properties and applications of mussel-inspired polydopamine. *J. biomed. Nanotechnol.* **2014**, 10 (10), 3063-3084.

25. Liu, Y.-C.; Jang, L.-Y. Relationship between crystalline orientations of gold and surface-enhanced raman scattering spectroscopy of polypyrrole and mechanism of roughening procedure on gold via cyclic voltammetry. *J. Phys. Chem. B* **2002**, 106 (26), 6748-6753.

26. Liu, Y.-C.; Peng, H.-H. Fabricating gold nanocomplexes of controllable size using electrochemical oxidation−reduction cycling of gold substrates in aqueous solution. *J. Phys. Chem. B* **2004**, 108 (43), 16654-16658.

27. Shaw III, C. F.; Schaeffer, N.; Elder, R.; Eidsness, M.; Trooster, J. M.; Calis, G. H. Bovine serum albumin-gold thiomalate complex: Gold-197 moessbauer, exafs and xanes, electrophoresis, sulfur-35 radiotracer, and fluorescent probe competition studies. *J. Am. Chem. Soc.* **1984**, 106 (12), 3511-3521.

28. Williams, D.; Askill, I.; Smith, R. Protein adsorption and desorption phenomena on clean metal surfaces. *J. biomed. Mater. Res.* **1985**, 19 (3), 313-320.

29. Tsai, D.-H.; DelRio, F. W.; Keene, A. M.; Tyner, K. M.; MacCuspie, R. I.; Cho, T. J.; Zachariah, M. R.; Hackley, V. A. Adsorption and conformation of serum albumin protein on gold nanoparticles investigated using dimensional measurements and in situ spectroscopic methods. *Langmuir* **2011**, 27 (6), 2464-2477.

30. Sakata, T.; Miyahara, Y. Detection of molecular charges at cell membrane. *Jpn. J. Appl. Phys.* **2008**, 47 (1R), 368-370.

31. Sakata, T.; Sugimoto, H. Continuous monitoring of electrical activity of pancreatic β-cells using semiconductor-based biosensing devices. *Jpn. J. Appl. Phys.* **2011**, 50 (2R), 020216.

32. Otsuka, H.; Nagamura, M.; Kaneko, A.; Kutsuzawa, K.; Sakata, T.; Miyahara, Y. Chondrocyte spheroids on microfabricated peg hydrogel surface and their noninvasive functional monitoring. *Sci. Technol. Adv. Mater.* **2012**, 13 (6), 064217.

33. Sakata, T.; Saito, A.; Mizuno, J.; Sugimoto, H.; Noguchi, K.; Kikuchi, E.; Inui, H. Single embryo-coupled gate field effect transistor for elective single embryo transfer. *Anal. Chem.* **2013**, 85 (14), 6633-6638.

34. Lee, H.; Rho, J.; Messersmith, P. B. Facile conjugation of biomolecules onto surfaces via mussel adhesive protein inspired coatings. *Adv. Mater.* **2009**, 21 (4), 431-434.

35. Ku, S. H.; Lee, J. S.; Park, C. B. Spatial control of cell adhesion and patterning through mussel-inspired surface modification by polydopamine. *Langmuir* **2010**, 26 (19), 15104-15108.

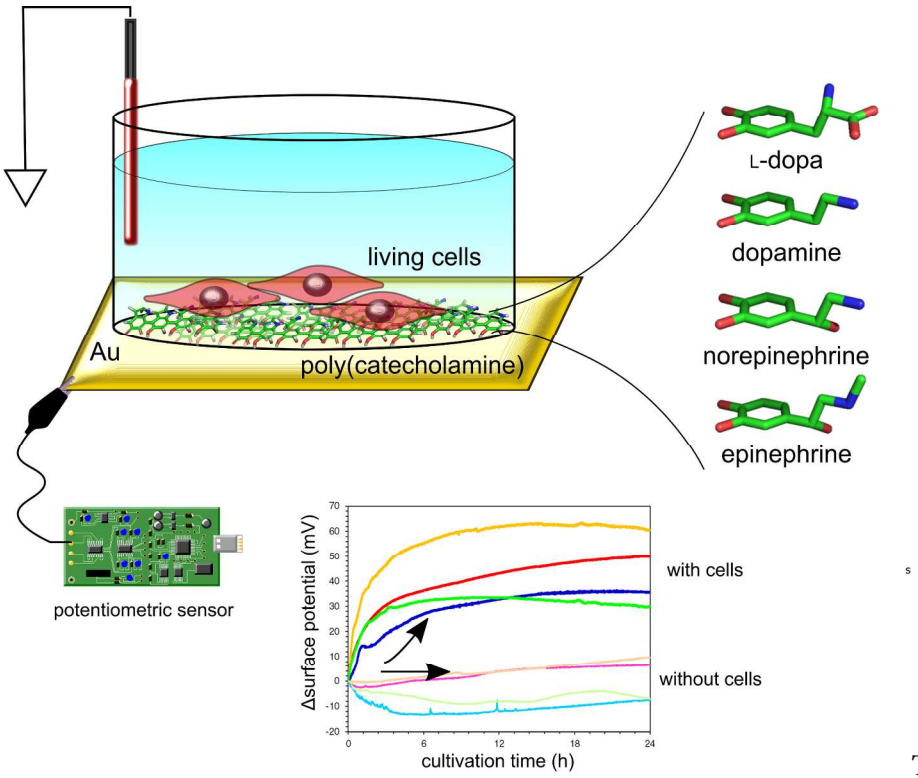


Table of Contents

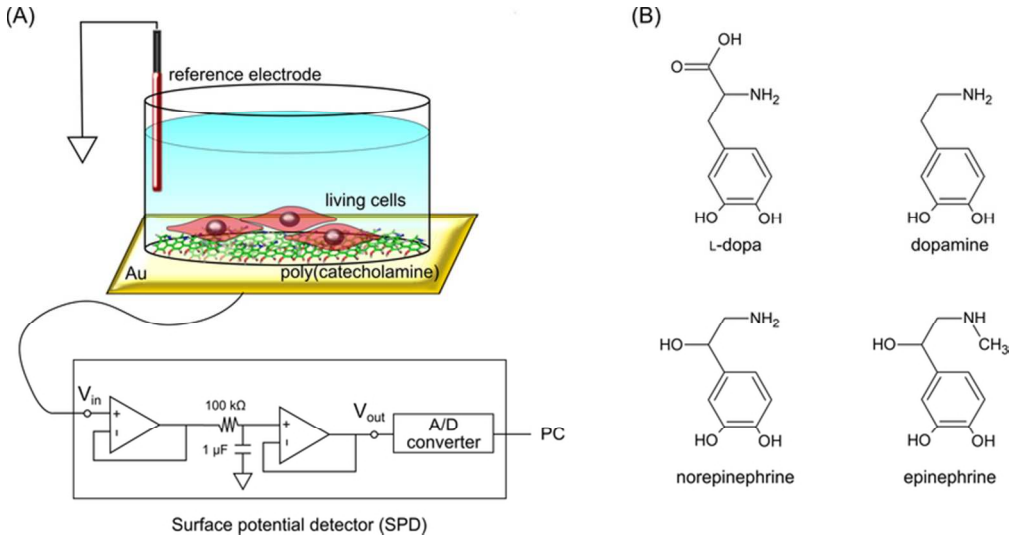


Figure 1 (A) Schematic illustration of cell sensing device in this study. A pCA nanolayer was deposited on an Au substrate and the changes in its interfacial charge were detected by a SPD comprising a voltage fol-lower circuit and an AC/DC signal converter. (B) Chemical structure of four types of pCA: LD, DA, NE, and EP.

70x36mm (300 x 300 DPI)

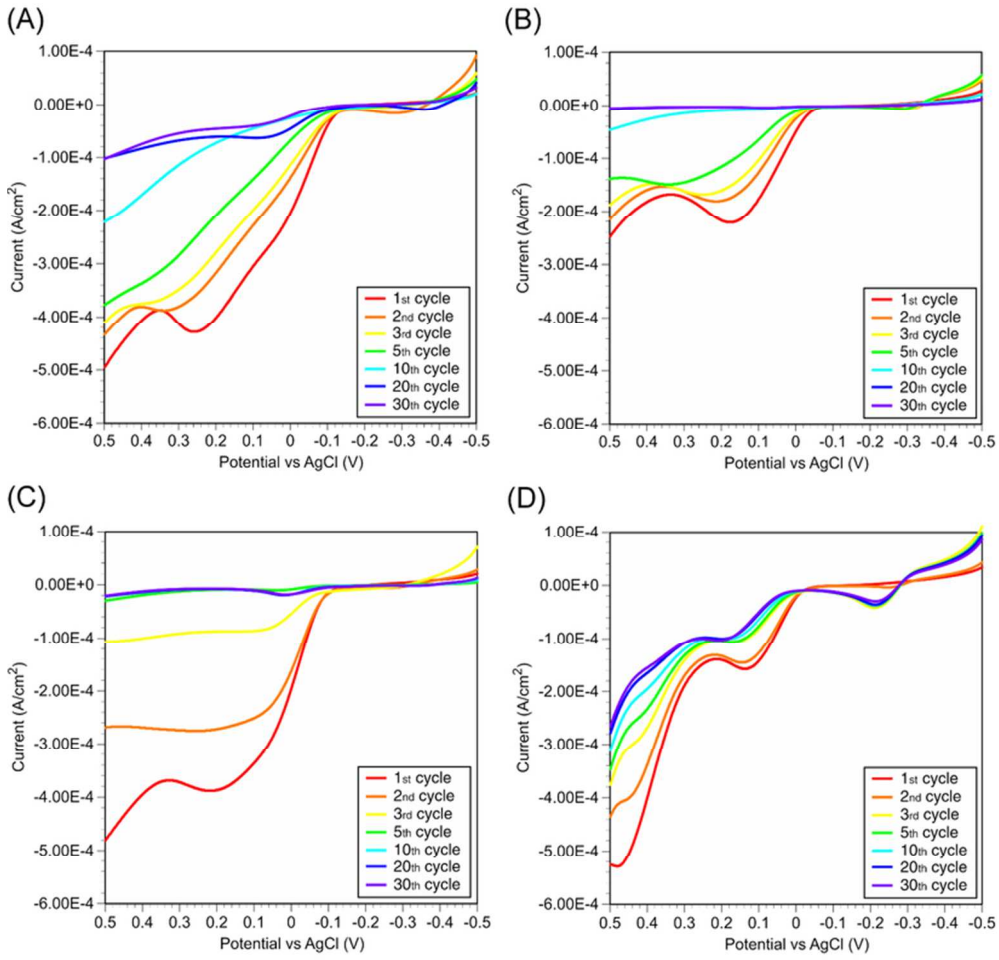


Figure 2 Cyclic voltammograms of the four types of catecholamine deposited by electropolymerization on an Au surface as a working elec-trode, with platinum as a counter electrode and Ag/AgCl as a reference electrode. Each catecholamine was dissolved in degassed 100 mM Tris buffer. The potential was swept in the forward direction from −0.5 to +0.5 V at a scan rate of 0.02 V/s for 30 cycles. (a) L-dopa, (b) dopamine, (c) norepinephrine, and (d) epinephrine.

70x67mm (300 x 300 DPI)

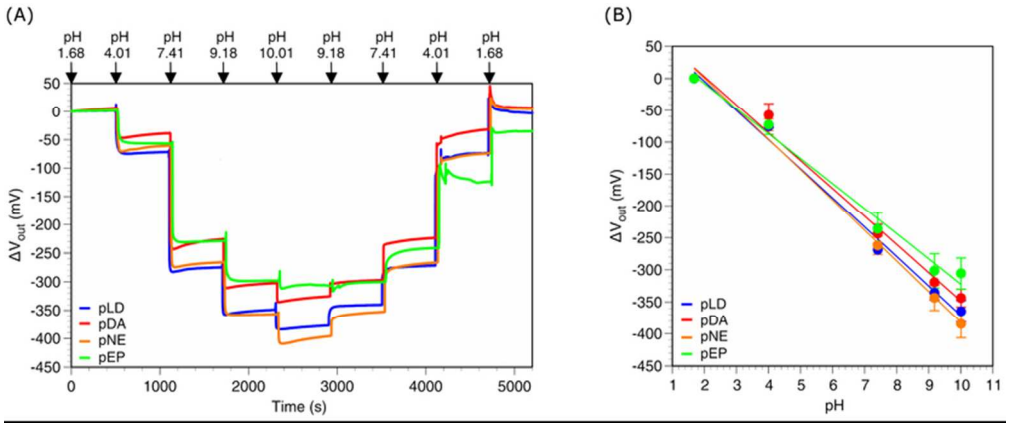


Figure 3 (A) Time course for the change in the surface potential of each type of pCA with solution pH from 1.68 to 10.01. The pH was increased from 1.68 to 10.01 then reduced to 1.68 (B) Linear plot of ion voltage shift against pH obtained using pCA-coated SPD. The data are based on the electrical signals shown in Figure 3A. The initial volt-age was set to 0 mV at pH 1.68.

70x29mm (300 x 300 DPI)

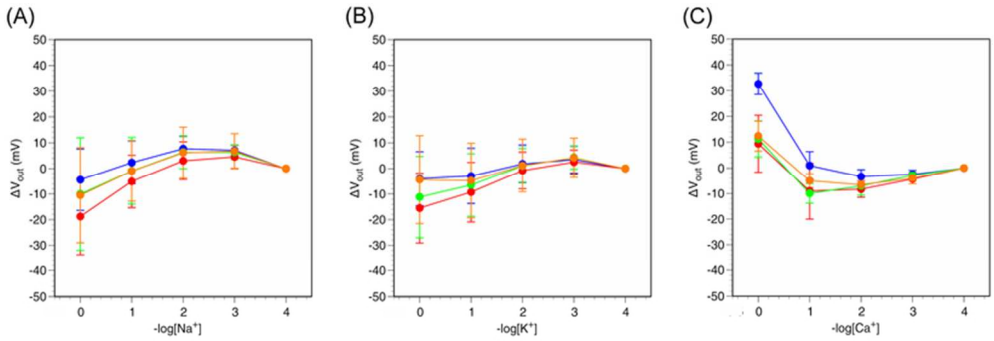


Figure 4 Change in output voltage ($V_{out}$) plotted against logarithm of $Na^+$, $K^+$, and $Ca^{2+}$ concentrations for each pCA-coated Au electrode (blue: pLD, red: pDA, orange: pNE, green: pEP). The concentration of each ion was varied from 100 μM to 1 M. The pH of each solution was fixed at 7.4. The initial voltage was set to 0 mV at a concentration of 100 μM.

70x23mm (300 x 300 DPI)

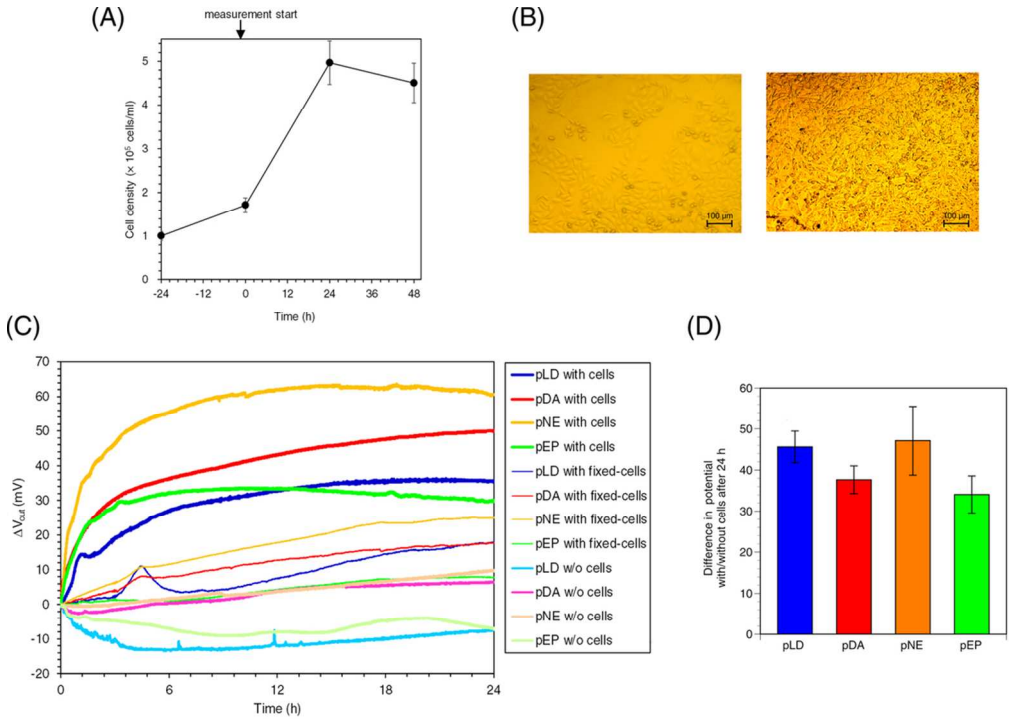


Figure 5 (A) Growth rate of the HeLa cells after seeding of $1.0 \times 10^5$ cells/ml. (B) The images of the proliferation of HeLa cells on the pDA-coated SPD cultivated after 0 h (left) and 24 h (right). (C) Time course for the change in potential ($\Delta V_{out}$) at pCA-modified Au electrodes with and without HeLa cells during cultivation. Changes in the output voltage are shown for pLD-modified Au with cells (blue line) and without cells (light blue line), pDA-modified Au with cells (red line) and with-out cells (light red line), pNE-modified Au with cells (orange line) and without cells (light orange line), and pEP-modified Au with cells (green line) and without cells (light green line). (D) Difference in potential for each pCA-coated SPD with and without cells after 24 h.

99x70mm (300 x 300 DPI)

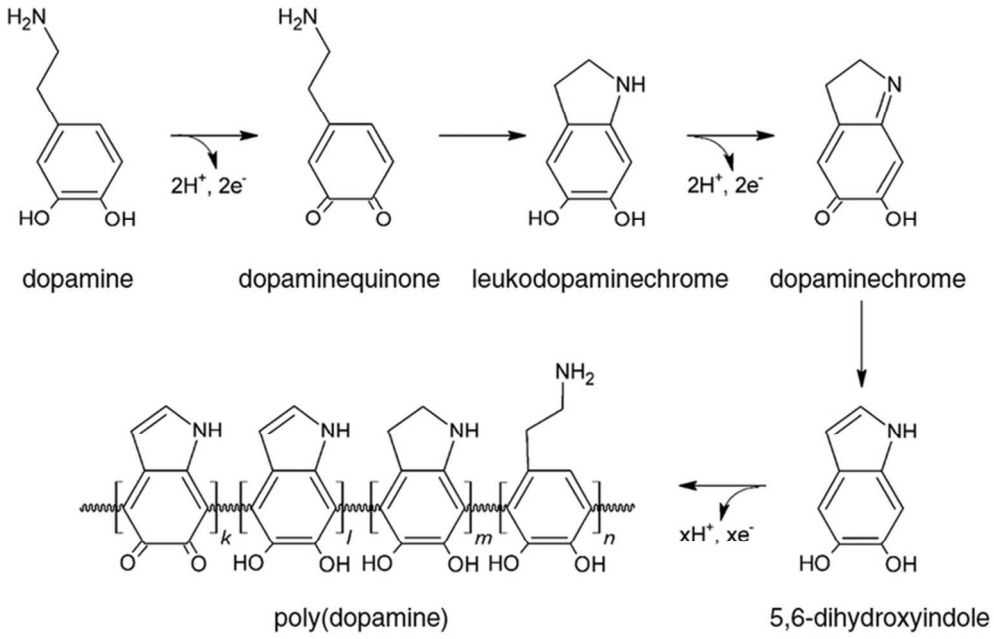


Scheme 1 Proposed oxidative pathway from dopamine to poly(dopamine). Four electrons were generated from the starting material (dopamine) to the precursor of pDA (5,6-dihydroxyindole).

70x44mm (300 x 300 DPI)